Multistep Phosphorylation by Oncogenic Kinases Enhances the Degradation of the NF2 Tumor Suppressor Merlin[1]

Minja Laulajainen*, Taru Muranen*, Tuula A. Nyman[†], Olli Carpén*,[‡] and Mikaela Grönholm*,[§]

*Biomedicum Helsinki, Department of Pathology, University of Helsinki, Helsinki, Finland; [†]Protein Chemistry Research Group, Institute of Biotechnology, University of Helsinki, Helsinki, Finland; [‡]Department of Pathology, University of Turku and Turku University Central Hospital, Turku, Finland; [§]Division of Biochemistry and Biotechnology, Department of Biosciences, University of Helsinki, Helsinki, Finland

Abstract

Mutations in the *Neurofibromatosis 2* gene (*NF2*) predispose to tumors of the nervous system, mainly schwannomas and meningiomas. The *NF2* gene encodes for the tumor suppressor protein merlin (moesin-ezrin-radixin–like protein), which functions as a linker between the plasma membrane and the cytoskeleton. Carboxyterminal phosphorylation affects merlin activity, but many open questions on the regulation of merlin function still remain. The phosphoinositide 3-kinase/Akt pathway is activated in human vestibular schwannoma, suggesting a role for Akt-dependent merlin regulation in the formation of these tumors. In this study, we identify merlin serine 10 as a novel substrate for Akt phosphorylation. We demonstrate that this N-terminal phosphorylation directs merlin for proteasome-mediated degradation and affects merlin binding to the E3 ligase component DCAF1. Our data indicate that sequential phosphorylation of merlin C- and N-terminus by different oncogenic kinases targets merlin for degradation and thus downregulates its activity. On the basis of these findings, we propose a model for a posttranslational mechanism of merlin inactivation.

Introduction

The NF2 tumor suppressor merlin, encoded by the *NF2* gene, regulates proliferation in many cell types [1]. Merlin belongs to the ERM (ezrin-radixin-moesin) family of proteins that all function as linkers between the cell membrane and cytoskeleton [2]. Like the other ERM proteins, merlin can also form intramolecular N- to C-terminal associations known to affect its activity [3–5]. The function of merlin is regulated through phosphorylation of a C-terminal serine 518 (S518), which is a substrate for both p21-activated kinase (PAK) and protein kinase A (PKA) [6–9]. Phosphorylation of S518 is predicted to unfold merlin and lead to reduced inhibition of cell growth, whereas dephosphorylation of S518 by the moesin phosphatase MYPT-1-PP1δ activates the tumor suppressor function of merlin leading to growth arrest [10,11]. However, the exact mechanism by which S518 phosphorylation regulates merlin's tumor-suppressive activity is still open. In addition to the C-terminal serine, merlin is phosphorylated by PKA on serine 10 (S10), which leads to modulation of the actin cytoskeleton [12].

The serine/threonine kinase Akt (protein kinase B) regulates many cellular processes such as motility, growth, and apoptosis. The phospho-inositide 3-kinase (PI3K)/Akt signaling pathway is growth-promoting in many human malignancies, and overexpression or hyperactivation of Akt is often associated with tumor development [13]. Three genes encode for the mammalian Akt isoforms: *PKBα* (Akt1), *PKBβ* (Akt2), and *PKBγ* (Akt3). Akt1 is ubiquitously expressed at high levels; Akt2

is highly expressed in insulin-sensitive tissues such as liver, skeletal muscle, and adipose tissue; whereas the highest expression of Akt3 is seen in the brain and testis [14]. The Akts are regulated by phosphoinositide-dependent kinase 1 (PDK1), which acts downstream of PI3K and phosphorylates Akt on threonine 308 in its activation loop [15], but full activation of Akt requires additional phosphorylation on serine 473 [16].

Activation of the PI3K/Akt pathway has been implicated in survival of Schwann cells [17] that are susceptible to tumor formation in the NF2 disease, and several studies indicate an interplay between merlin and Akt. Merlin plays a role in controlling the PI3K/Akt pathway by inhibiting Akt signaling [18,19], and the pathway is activated in both human schwannoma [20–22] and in malignant mesotheliomas from Nf2 +/− mice [23]. Recently, Akt-mediated phosphorylation of merlin was also described [24], but there are still open questions about the biologic effects of Akt on merlin.

In this report, we have studied the phosphorylation of merlin and identified S10 as an Akt phosphorylation site. Our results show that this N-terminal phosphorylation directs merlin for proteasome-mediated degradation thereby affecting merlin function. These findings implicate a mechanism, by which the oncogenic Akt pathway can regulate cell growth.

Materials and Methods

Cells, Plasmids, and Antibodies

COS-7 cells were maintained in Dulbecco minimum essential medium (Gibco-Invitrogen, Carlsbad, CA) with 10% fetal bovine serum (PromoCell, Heidelberg, Germany) and antibiotics.

For the expression of recombinant GST-merlin fusion proteins, merlin fragments 1-100, 1-314, 314-477, 1-547, and 492-595 in pGEX4T1 vector (Amersham Biosciences, Uppsala, Sweden) were used. Human merlin isoform I (WT, amino acids 1-595) in pcDNA3 vector (Invitrogen) was used for transfection experiments. The point mutations S10A, S10D, T230A, S315A, S518A, and S518D were made by site-directed mutagenesis in both vectors using the QuikChange Kit (Stratagene, La Jolla, CA). The authenticity of all constructs was verified by sequencing. Akt WT in pUSEamp vector was from Upstate Biotechnology (Temecula, CA). The cDNAs of bovine myristoylated Akt and myristoylated kinase-dead Akt were kind gifts from Dr Rene H. Medema. Both constructs contain N-terminal myristoylation signals, and the Akt KD construct has a K179A mutation in the catalytic domain. The DCAF1 in pRK5 vector was obtained from Dr Filippo Giancotti and had been described [25].

Antimerlin pAb A-19 sc-331 (Santa Cruz Biotechnology, Santa Cruz, CA) and KF10 monoclonal antibody (mAb) [26] were used to detect merlin. S518 phosphorylated merlin was detected with pS518 pAb (Biodesign, Saco, ME). Rabbit polyclonal antibody recognizing human merlin phosphorylated on S10 was produced by immunization of a 11-mer synthetic phosphopeptide IASRM(pS)FSSLK and subsequent purification of the antiserum using both negative and positive affinity purification methods. The specificity of the antibody was tested against *in vitro* Akt-phosphorylated GST-merlin with and without S10A mutations. Rabbit monoclonal pan-Akt and phospho-Ser473 Akt antibodies (Cell Signaling Technology, Danvers, MA) were used for Akt detection, phospho-GSK-3α/β (Ser21/9) (Cell Signaling Technology) and GSK-3α (Santa Cruz Biotechnology) antibodies were used for GSK3 detection, and anti-VprBP antibody (SMS-Gruppen, Rungsted, Denmark) was used for DCAF1 detection. The Ub (P4G7) antibody (Santa Cruz Biotechnology) was used for monoubiquitin and

polyubiquitin detection. GST fusion proteins were detected with GST Ab (GE Healthcare, Uppsala, Sweden), and tubulin with α-tubulin mAb (Sigma-Aldrich, St Louis, MO). Alexa-488– and Alexa-594–conjugated goat antimouse and goat antirabbit antibodies (Invitrogen-Molecular Probes) were used as secondary antibodies in immunofluorescence, and horseradish peroxidase–conjugated rabbit antimouse, swine antirabbit (DAKO A/S, Glostrup, Denmark), and swine antigoat (Santa Cruz Biotechnology) secondary antibodies were used in Western blot analysis.

Transfections, Immunofluorescence, and Immunoblot Analysis

Cells were transfected using FuGENE 6 transfection reagent (Hoffmann-La Roche Ltd, Basel, Switzerland) and incubated for 48 hours before analysis. For Akt kinase activation and inhibition experiments, cells were cultured in serum-free medium for 24 hours and treated before lysis with 0.2 μg/ml human recombinant EGF (Calbiochem, La Jolla, CA) for 10 minutes, with 50 μM LY-294002 (Sigma-Aldrich) for 1 hour or with 0.1 μM Calyculin A (Calbiochem) for 10 minutes all at 37°C. For degradation assays, serum-starved cells were treated for 24 hours (or 3 hours for ubiquitination experiment) with 5 μM of the proteasomal inhibitor MG132 or 0.1 μM of Bafilomycin A1 (both from Sigma-Aldrich) used to inhibit lysosomal function. To activate or inhibit endogenous PKA activity, cells were treated with 50 mM IBMX and 25 mM forskolin or 10 μM H89 (all from Sigma-Aldrich) for 24 hours. For Western blot analysis of fractionated lysates, cells were rinsed with phosphate-buffered saline and lysed in ELB buffer (50 mM HEPES, pH 7.4, 150 mM NaCl, 5 mM EDTA) containing 0.5% Nonidet P-40 (NP-40), HALT phosphatase inhibitors (Pierce, Rockford, IL), and complete protease inhibitors (Roche). Lysed cells were centrifuged at 13,000*g* for 20 minutes at +4°C, and the pellet and supernatant were resolved in equal amounts of reducing Laemmli buffer. Whole-cell lysates were prepared by adding reducing Laemmli sample buffer on the plates. Samples were resolved on SDS-PAGE, transferred to nitrocellulose filters, and analyzed by immunoblot analysis with appropriate antibodies using enhanced chemiluminescence detection (Amersham Biosciences). For immunofluorescence, cells grown on glass coverslips were fixed in 3.5% paraformaldehyde (pH 7.5) and detected with appropriate antibodies using standard protocols.

Immunoprecipitation

COS-7 cells were lysed 48 hours after transfection in ELB buffer containing 0.5% NP-40, HALT phosphatase inhibitors, and complete protease inhibitors. Lysed cells were centrifuged at 13,000*g* for 30 minutes at 4°C. The supernatants were diluted 1:1 to ELB buffer without NP-40 and precleared with G-sepharose beads for 1 hour at 4°C. Beads were spun down, and cleared supernatants were incubated with appropriate antibodies overnight at 4°C under rotation. G-Sepharose beads were added and the samples were incubated for additional 4 hours at 4°C under rotation. Immunoprecipitates were washed with ELB buffer, and bound proteins were eluted from the beads by boiling in nonreducing Laemmli buffer and analyzed by immunoblot analysis.

In Vitro *Phosphorylation of Merlin*

GST fusion proteins were expressed in *Escherichia coli* DH5α and purified. Glutathione-Sepharose beads (Amersham Biosciences) to which ~4 μg of fusion protein was conjugated were washed in Akt buffer (50 mM Tris-HCl, pH 7.5, 0.1 mM EGTA, 15 mM DTT, 15 mM MgCl$_2$, 100 μM ATP) or PKC buffer (1/5 PKC lipid activator [Upstate Biotechnology], 20 mM HEPES, 10 mM MgCl$_2$,

0.1 mM EGTA, 500 µM ATP) containing complete protease inhibitors. The phosphorylation reaction was carried out in a 30-µl buffer volume including 10 µCi of [γ-^{33}P] ATP (PerkinElmer Life Sciences, Waltham, MA) and 0.1 µg of human recombinant active Akt1 (ΔPH, S473D), Akt2 (δPH, S474D), Akt3 (117-end, S472D; Upstate Biotechnology) or 5 ng of human recombinant PKC theta (Invitrogen) for 30 minutes at 30°C. Beads were washed in kinase buffer, reducing Laemmli buffer was added, and samples were resolved by SDS-PAGE. The gel was fixed and stained by Coomassie Blue followed by exposure to a PhosphoImager plate and detection with Typhoon Imager 9400 (both from GE Healthcare). For *in vitro* kinase assays of the full-length protein, COS-7 cells were transfected with merlin constructs, and expressed proteins were immunoprecipitated with the C-terminal merlin KF10 mAb. Immunoprecipitated proteins were phosphorylated *in vitro* by Akt1 as described previously.

Mass Spectrometry Analysis

Merlin was immunoprecipitated from serum-starved transfected COS-7 cells that were either EGF stimulated as described previously or cotransfected with Akt myr. For identification, the immunoprecipitated proteins were separated by SDS-PAGE and visualized with silver staining [27], after which the protein bands were cut out from the gel, in-gel digested with trypsin into peptides, and analyzed by liquid chromatography–tandem mass spectrometry (LC-MS/MS) using an Ultimate 3000 nano-LC (Dionex, Sunnyvale, CA) and a QSTAR Elite hybrid quadrupole TOF-MS (Applied Biosystems/MDS Sciex, Foster City, CA) with nano–electrospray ionization as previously described [28–30].

The LC-MS/MS data were searched with in-house Mascot version 2.2 through ProteinPilot 2.0.1 interface against a self-made database containing merlin sequence (SwissProt entry P35240). In addition, searches were done against SwissProt database (version 57.10; 512,205 sequences). The search criteria for Mascot searches were the following: trypsin digestion with three missed cleavages allowed, carbamidomethyl (C) as fixed modification and oxidation (M), phospho (ST), phospho (Y) as variable modifications. For the LC-MS/MS spectra, the maximum precursor ion mass tolerance was 50 ppm, and MS/MS fragment ion mass tolerance of 0.2 Da and peptide charge state of +1, +2, or +3 were used.

Affinity Pull-down

Transfected COS-7 cells were lysed in cold binding buffer (140 mM NaCl, 1 mM Tris, pH 7.5) containing 0.5% Triton X-100 and complete protease inhibitors, and the homogenates were cleared by centrifugation at 4°C for 20 minutes at 13,000*g*. G-Sepharose beads carrying ~4 µg of bacterially produced GST fusion proteins were washed in binding buffer and incubated with the lysates overnight at 4°C under rotation. Samples were washed with binding buffer, and the bound proteins were separated by SDS-PAGE, blotted, and detected with the appropriate antibody. The blot was further stripped and reprobed with GST Ab to verify equal amounts of proteins on the beads.

Quantifications

ImageQuant TL2003 software (GE Healthcare) was used to analyze band intensities from immunoblots. Merlin intensities were normalized to α-tubulin to obtain the merlin-tubulin ratio or the p-S518 amount to total merlin to obtain the p-S518–merlin ratio. For quantification of *in vitro* phosphorylation, the phospho-signal from the autoradiograph read by Typhoon Imager 9400 was analyzed by ImageQuant TL2003

and normalized to the Coomassie Blue staining, and the background radioactivity (untransfected cells) was subtracted from merlin samples. All quantifications were done from at least three independent experiments, and Student's *t* test was used for calculation of *P* values. In figures, mean ± SD is given.

Results

Merlin Is Phosphorylated on Serine 10 by All Akt Isoforms

To study the putative link between merlin and Akt, we first performed an *in vitro* Akt phosphorylation assay with recombinant merlin fragments. Full-length merlin (residues 1-595) is easily degraded when produced as a GST fusion in bacteria; therefore, merlin 1-547 and merlin 492-595 were used to cover the entire molecule. The Akt substrate region in merlin was mapped to the very N-terminus of the protein, as merlin 1-100 was phosphorylated by Akt1 *in vitro* (Figure 1*A*). Akt did not phosphorylate merlin C-terminus (492-595) in contrast to the previously characterized merlin phosphorylating kinases, PAK and PKA. Substitution of serine 10, previously identified as a substrate for PKA [12], abrogated the phosphorylation in all merlin constructs, showing that S10 is required for Akt phosphorylation. To test whether merlin serves as a substrate for all AGC kinases, a subfamily of protein kinases to which both PKA and Akt belong, a protein kinase C (PKC) phosphorylation assay was performed. PKC phosphorylates merlin N-terminus *in vitro*, but the S10A mutation does not affect the phosphorylation (Figure 1*B*). Therefore, it is unlikely that the diminished phosphorylation of S10A constructs by Akt would result from general misfolding of the merlin proteins.

Merlin threonine 230 and serine 315 were recently described as Akt phosphorylation sites [24]. To test phosphorylation of these residues and to confirm S10 phosphorylation in full-length merlin, the Akt *in vitro* kinase assay was performed with full-length merlin with or without alanine substitutions (S10A, T230A, S315A) in different combinations, immunoprecipitated from transfected COS-7 cells. Alanine substitution of threonine 230 and serine 315 had no effect on Akt phosphorylation, whereas S10A mutation resulted in loss of phosphorylation in all constructs (Figure 1*C*). These results indicate that S10 is the sole target of Akt. To further confirm S10 phosphorylation, a phospho-specific antibody against phospho-S10 was raised. The phospho-S10 Ab recognized GST-merlin 1-547 phosphorylated by Akt, whereas S10A-containing constructs or unphosphorylated merlin was not detected by the antibody (Figure 1*D*).

To rule out that the conflicting results between our study and those published before were due to the use of different Akt isoforms, we studied the effect of the three kinases on merlin phosphorylation. The merlin 1-547 constructs were similarly phosphorylated by all isoforms, and mutation of S10 was sufficient to abolish the phosphorylation (Figure 1*E*). However, phosphorylation was not affected by the T230A and S315A mutations.

Finally, to study whether merlin S10 is an Akt substrate *in vivo*, merlin was expressed in COS-7 cells, which were either epidermal growth factor (EGF) stimulated to activate Akt or coexpressed with myristoylated Akt (Akt myr), a constitutively activated and membrane-targeted form of Akt. Merlin was immunoprecipitated, resolved in SDS-PAGE, and silver stained. Bands were subjected to proteolytic cleavage and analyzed by MS. Analysis of the EGF-stimulated merlin MS spectra revealed several phosphorylated peptides, among them the peptide corresponding to merlin residues 9-16 containing phospho-serine 10 (data not
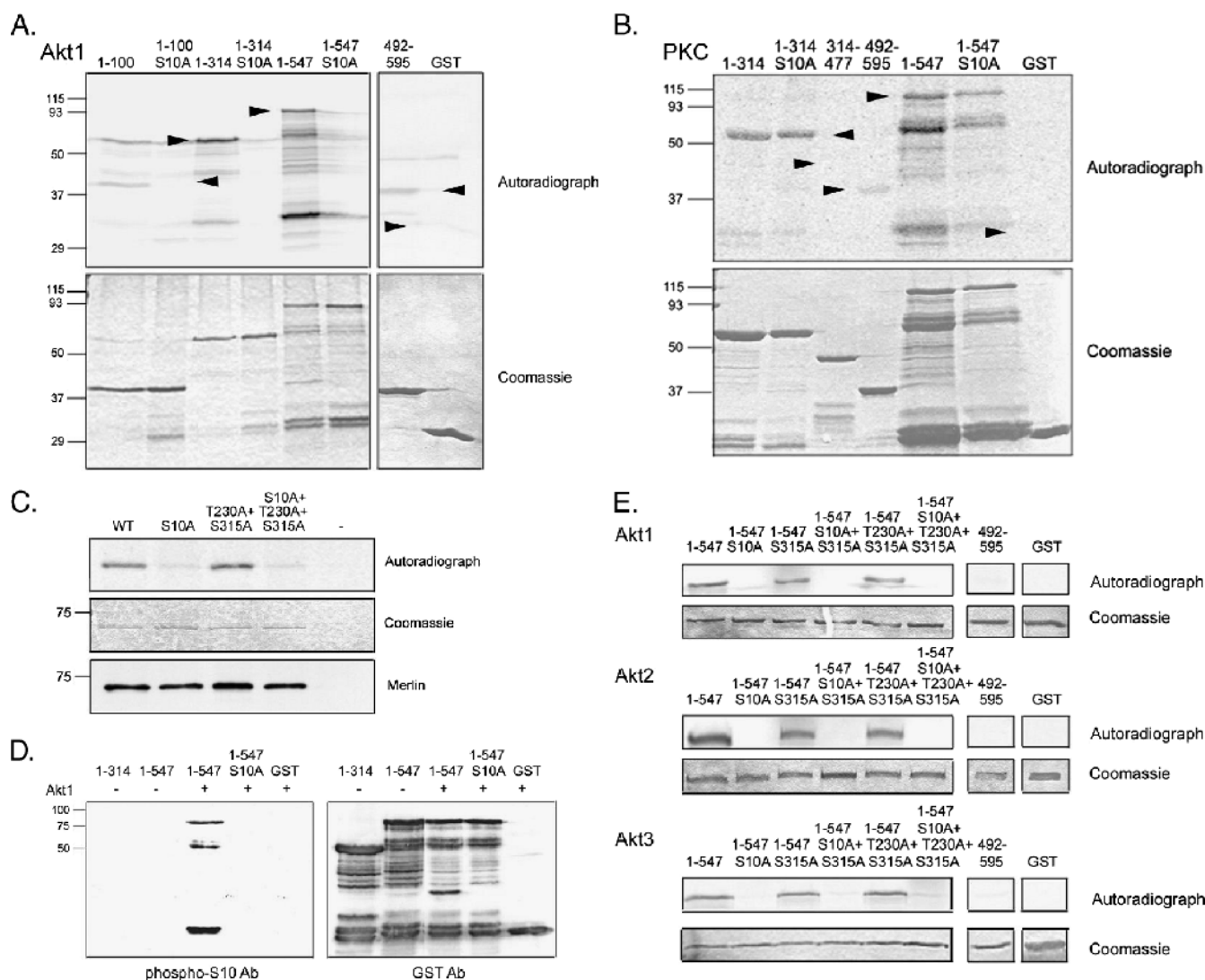
Figure 1. All Akt isoforms phosphorylate merlin at serine 10. (A) Recombinant GST-merlin fragments were Akt-phosphorylated *in vitro*, separated on SDS-PAGE and exposed (upper panel). The Coomassie Blue staining shows loading of the proteins (lower panel) and arrowheads mark the merlin GST constructs. Merlin 1-100, 1-314, and 1-547 are phosphorylated by Akt1, and the S10A substitution abolishes the phosphorylation. (B) GST-merlin fragments were phosphorylated *in vitro* by PKC, exposed (upper panel), and stained with Coomassie Blue (lower panel). Merlin 1-314 is phosphorylated by PKC, but S10A mutation does not affect the phosphorylation. (C) Full-length wild-type (WT) merlin and merlin mutants were expressed in COS-7 cells, immunoprecipitated, and subjected to an *in vitro* Akt kinase assay. Immunoprecipitation from untransfected cells (−) was used as a negative control. WT merlin is phosphorylated by Akt, whereas phosphorylation is decreased in both S10A-containing constructs (upper panel). Substitution of T230 or S315 does not affect phosphorylation. The Coomassie Blue staining shows equal loading (middle panel) and the lower panel shows immunoprecipitated merlin. (D) *In vitro* kinase assay with merlin GST proteins incubated with (+) or without (−) Akt1 was detected with phospho-S10 Ab (left panel) and GST Ab (right panel). The phospho-S10 antibody detects Akt1 incubated merlin 1-547 but not S10A or untreated 1-547. (E) GST-merlin fusion proteins were phosphorylated with Akt1, Akt2, and Akt3 kinases. Proteins were resolved on SDS-PAGE, stained with Coomassie Blue (lower panels), and exposed (upper panels). Merlin 1-547 is phosphorylated by all Akt isoforms, and the S10A mutation abolishes the phosphorylation. T230A and S315A substitutions have no effect on phosphorylation.

shown). Proteins from merlin and Akt myr–cotransfected cells were also studied, but interestingly, no phosphorylated peptides were detected in this sample.

Merlin and Akt Colocalize and Interact Both *In Vitro* and *In Vivo*

Although stable complex formation between the kinase and its substrate is not generally required for phosphorylation, many Akt substrates have been shown to form detectable complexes with the kinase. The interaction may promote substrate phosphorylation and/

or anchor Akt in different cellular compartments allowing localized signaling networks [31]. Because Akt-mediated phosphorylation of merlin was confirmed, colocalization between these proteins was studied. Merlin WT and S10A constructs were cotransfected with Akt1 into COS-7 cells, and the cells were treated with EGF or the PI3K inhibitor LY294002 to either activate or inactivate Akt. Both WT and S10A merlin colocalized with active Akt at the cell membrane in EGF-treated cells (Figure 2A, *upper and middle panels*). Akt1 showed nuclear staining in PI3K inhibitor–treated cells, whereas merlin was still present at the cell membrane (Figure 2A, *lower panels*). The same localization

pattern was detected in Nf2–/– mouse embryonic fibroblasts (data not shown).

To further investigate the interaction of merlin and Akt and to map the binding region, an affinity pull-down assay was performed. Merlin GST proteins were incubated with lysates from Akt1-transfected COS-7 cells, and the amount of bound Akt1 was analyzed. Figure 2B demonstrates that the FERM domain containing constructs 1-314 and 1-547 bind Akt1 *in vitro*, whereas the binding affinity to α-helical 314-477 and C-terminal 492-595 constructs was very weak. Because merlin 1-547 binding was stronger than the interaction observed with 1-314, it is possible that merlin 1-547 contains not only the N-terminal but also another more C-terminal binding site. Merlin S10 seems not to be critical for binding as S10A substitution bound Akt with similar affinity as WT.

To verify the binding, a coimmunoprecipitation assay with full-length merlin WT or S10A and Akt was performed from cotransfected COS-7 cell lysates. Our data show that merlin and Akt1 bind *in vivo* and confirm that the association is independent of the S10 phosphorylation (Figure 2C). Treatment of the cells with EGF did not change the binding affinity of merlin and Akt (data not shown).

Akt-Phosphorylated Merlin Is Degraded through a Proteasome-Dependent Pathway

In an attempt to further analyze serine 10 phosphorylation *in vivo*, merlin was immunoprecipitated from COS-7 lysates cotransfected with constitutively active Akt myr. Interestingly, significantly less merlin was detected in immunoprecipitates from cells in which Akt myr was overexpressed (data not shown). The low levels of merlin together with the MS analysis data, which showed that no phospho-peptides of merlin could be detected in Akt myr transfectants, suggested that merlin is degraded in response to Akt phosphorylation. To test this hypothesis, merlin WT and S10A were transfected into COS-7 cells together with either Akt myr or myristoylated kinase dead Akt (Akt KD). Akt KD–transfected cells were also treated with PI3K inhibitor to reduce endogenous Akt activity, and the Akt myr–transfected cells were incubated with the phosphatase inhibitor Calyculin A to increase the level of phosphorylated merlin. The phospho-Akt and phospho-GSK3 immunoblots confirm that Akt is activated in Akt myr–transfected cells (Figure 3A). Results show that the amount of WT merlin was significantly decreased and was, on an average, reduced by 65% in Akt myr–expressing cells compared with cells expressing
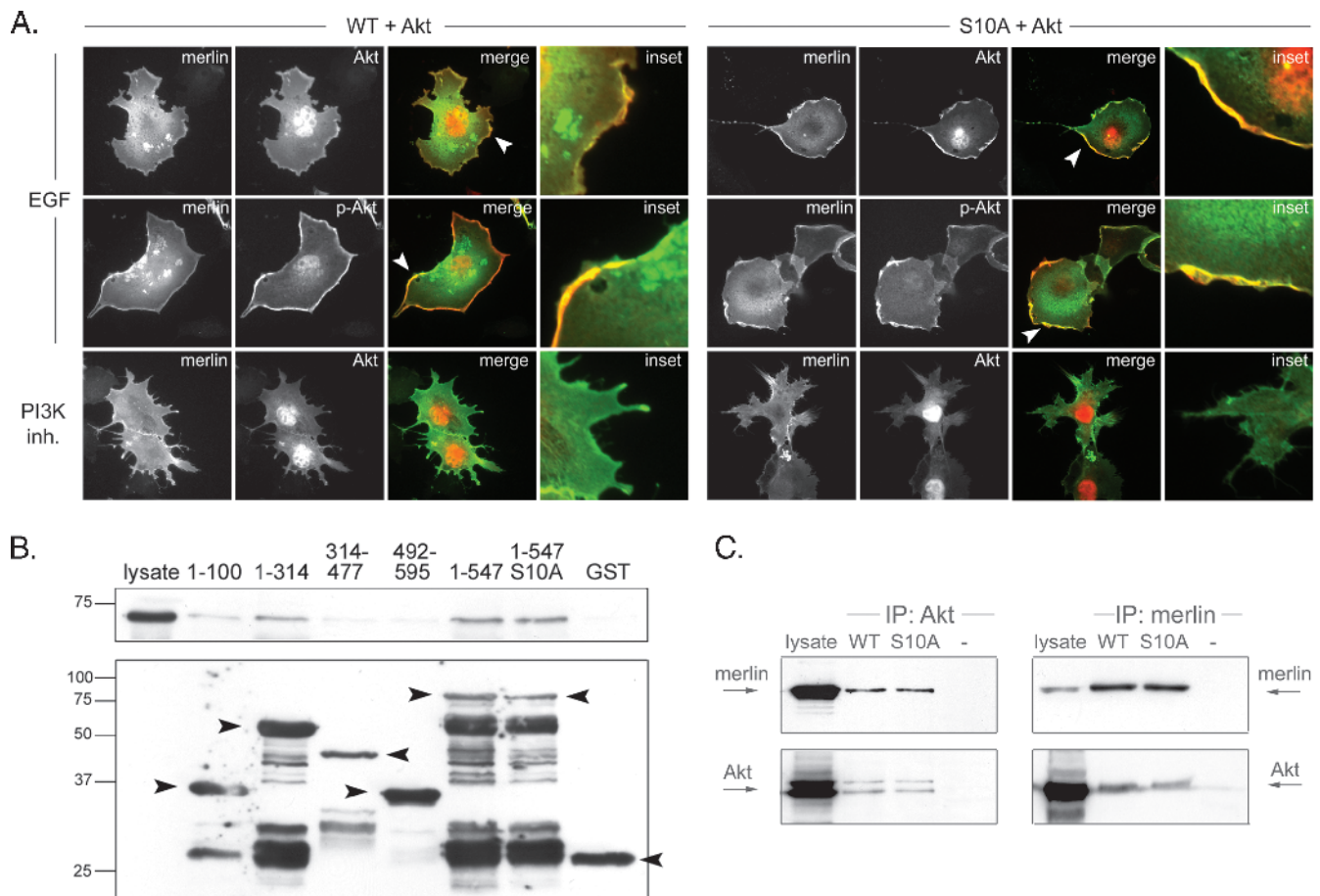
Figure 2. Merlin and Akt association *in vivo* and *in vitro*. (A) COS-7 cells were cotransfected with Akt1 and merlin WT or S10A and treated with EGF or LY294002 (PI3K inh.). Cells were stained for merlin (green) and Akt (red, top, and bottom) or phospho-Ser 473 Akt (p-Akt, red, middle). Merlin colocalizes with activated Akt at the cell membrane (arrowheads), and mutation of serine 10 does not affect merlin-Akt colocalization (right panel). (B) Glutathione bead–conjugated GST-merlin constructs were incubated with lysates from Akt1-transfected COS-7 cells and bound proteins were detected with Akt Ab (upper panel) and merlin with GST Ab (lower panel). Merlin N-terminus–containing fragments (1-100, 1-314, 1-547) bind Akt1 *in vitro*. The Akt binding affinity is not weakened by the S10A mutation. (C) Cotransfected merlin and Akt1 were coimmunoprecipitated from COS-7 cell lysates. Proteins were detected with merlin KF10 and pan-Akt antibodies and untransfected cells (−) were used as control. Both WT and S10A merlin interact with Akt1 *in vivo*.
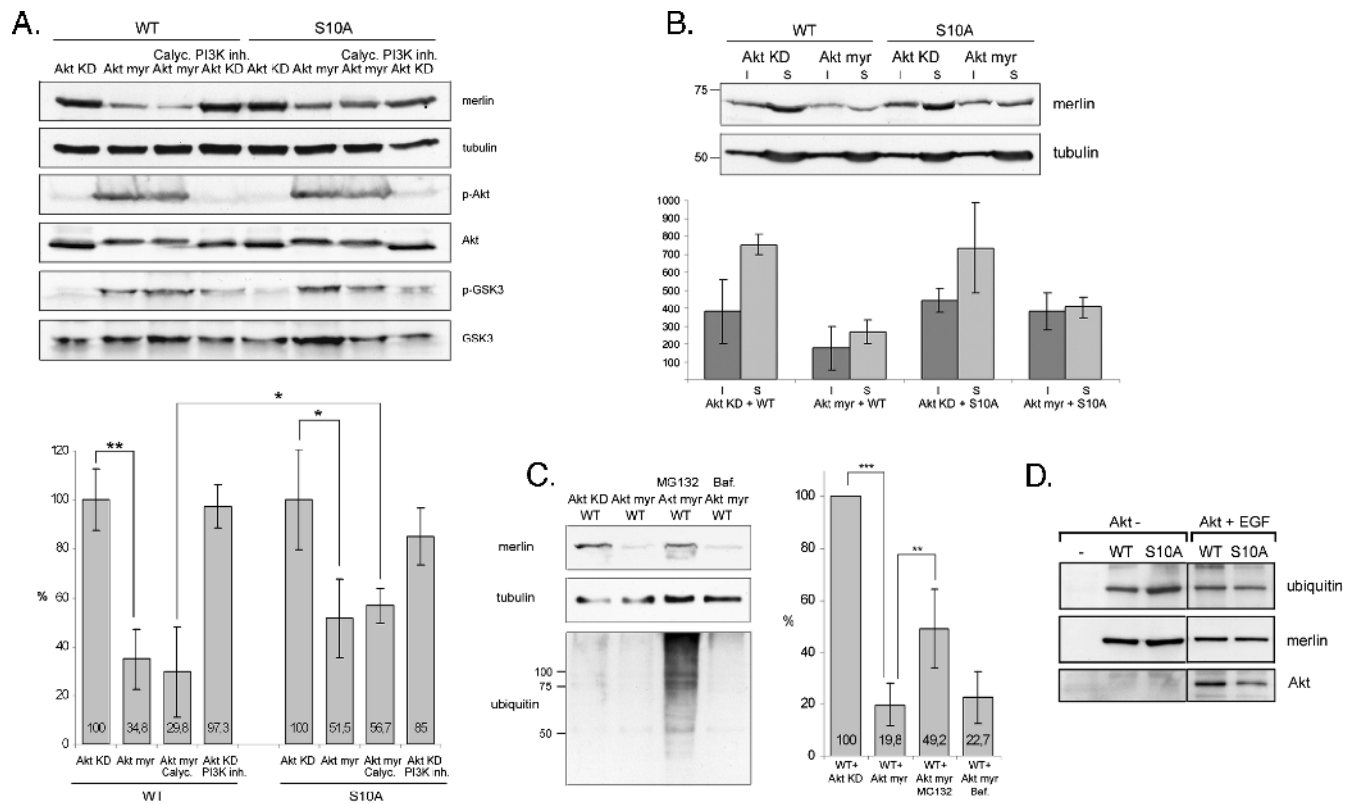
Figure 3. Constitutively active Akt degrades WT merlin through the proteasomal pathway. (A) COS-7 cells cotransfected with WT or S10A merlin and inactive (Akt KD) or constitutively active (Akt myr) Akt were untreated or treated with the phosphatase inhibitor Calyculin A (Calyc.) or PI3K inhibitor LY294002 (PI3K inh.). Lysates were run in SDS-PAGE and detected for merlin (A-19 Ab), phospho-Ser 473 Akt (p-Akt), Akt, phospho-GSK3 (p-GSK3), GSK3, and α-tubulin as a loading control. The merlin/tubulin ratio is shown in the lower chart and 100% represents the merlin level in Akt KD–expressing cells. The amount of WT merlin in cells expressing Akt myr is significantly decreased compared with cells expressing Akt KD, whereas S10A merlin is less sensitive to Akt myr coexpression. (B) Lysates from COS-7 cells cotransfected with merlin and Akt KD or Akt myr were separated into insoluble (I) and soluble (S) fractions and run in SDS-PAGE (upper panel). The merlin-tubulin ratio was quantified, and the amount of merlin in fractions is shown in arbitrary units (lower chart). Both the detergent-insoluble and -soluble WT merlin is degraded in Akt myr–transfected cells. (C) COS-7 cells were cotransfected with merlin WT and Akt KD or Akt myr. The WT + Akt myr–expressing cells were untreated or treated with MG132 or Bafilomycin A1 (Baf.), and lysates were detected with merlin A-19 Ab, α-tubulin Ab, and ubiquitin Ab (left panels). The merlin amount was quantified, and the level in WT + Akt KD–transfected cells was regarded as 100% (right chart). The proteasome inhibitor MG132 increases the amount of merlin in Akt myr–expressing cells. (D) WT and S10A merlin was immunoprecipitated from untransfected or Akt-transfected EGF-stimulated and MG132-treated COS-7 cells. Samples were detected for ubiquitin (upper panel) and merlin (middle panel). The expression of Akt was confirmed from the lysates with Akt antibody (lower panel). Merlin WT and S10A are equally ubiquitinated. **P < .01. *P < .05.

Akt KD (Figure 3A). Incubation with Calyculin A further increased the degradation of WT merlin. As expected, S10A merlin was more resistant to Akt myr–induced degradation than WT. The mild decrease detected in the amount of S10A merlin may be a result of the alanine substitution at S10, which does not fully mimic the unphosphorylated residue and is therefore not sufficient to completely inhibit degradation. Both the detergent-insoluble and -soluble WT merlin were degraded because of Akt myr overexpression (Figure 3B).

To determine the pathway that mediates the degradation of merlin, cells coexpressing merlin and Akt myr were treated with the proteasomal inhibitor MG132 or with Bafilomycin A1 to inhibit lysosomal function. The amount of merlin was quantified and compared with the level in untreated Akt KD–expressing cells. Treatment of cells expressing Akt myr and merlin with MG132 increased the amount of merlin from 20% in untreated cells to an average of 49%, whereas Bafilomycin A1 had no significant effect on the merlin level (Figure 3C). These results indicate that Akt-phosphorylated merlin is degraded through the proteasomal pathway. Proteins targeted for proteasomal

degradation are tagged with ubiquitins. To analyze the ubiquitination of merlin, immunoprecipitated WT and S10A merlin from MG132 treated COS-7 cells were immunoblotted for ubiquitin (Figure 3D). Both WT and S10A merlin are monoubiquitinated independently of Akt, but soluble polyubiquitinated merlin was not detected.

C-terminal Phosphorylation of Merlin Increases Serine 10 Phosphorylation

Because both Akt and PKA phosphorylate merlin S10, we next looked at the interplay between PKA and Akt and their effect on merlin degradation. Merlin WT was cotransfected into COS-7 cells with either Akt KD or Akt myr. The Akt myr–transfected cells were treated with the PKA inhibitor H89 to inhibit endogenous PKA activity or with forskolin and IBMX to activate PKA. The results show that Akt-induced merlin degradation is not PKA dependent because merlin is also degraded in H89-treated cells (Figure 4A). However, coactivation of Akt and PKA has an additive effect on merlin degradation.

Phosphorylation of S518 is known to regulate the tumor-suppressive activity of merlin. To study the interplay between the N- and C-terminal phosphorylation sites, an Akt kinase assay was conducted. Merlin full-length constructs with serine-to-alanine substitutions produced in COS-7 cells were immunoprecipitated, and bound proteins were phosphorylated *in vitro* by Akt. Because the merlin constructs were produced in COS-7 cells, the proper conformation of the proteins should be retained. The chart in Figure 4B shows the quantification of autoradiographs when the signal in merlin WT was regarded as 100%. In merlin S518D, mimicking the phosphorylated form, Akt phosphorylation of S10 was significantly increased compared with WT. Consequently, S10 phosphorylation of S518A merlin was lower than WT.

Mutation of T230 and S315 were shown to influence merlin function [24,32]. Although we could not detect Akt phosphorylation of these residues, their possible effect on merlin phosphorylation was analyzed. COS-7 cells were transfected with the mutants and lysates were detected with the phospho-S518 merlin Ab. Interestingly, alanine substitutions of T230 and S315 abrogated C-terminal S518 phosphorylation of merlin (Figure 4C).

Serine 10 Modifications Affect Binding of Merlin to DCAF1

The attachment of ubiquitins on proteins marked for proteasomal degradation is catalyzed by ubiquitin ligases. An interaction with VprBP/DCAF1 (DDB1- and Cul4-associated factor 1) has been shown to target merlin to the Roc1-Cul4A-DDB1 E3 ligase complex leading to merlin's polyubiquitination and proteasome-dependent degradation [33]. As our assays indicated that merlin is degraded through the proteasome in response to N-terminal phosphorylation, we studied whether phosphorylation of serine 10 targets merlin to the E3 ligase complex, directing it for degradation.

Merlin interacts with DCAF1 through its N-terminus [25,33]. To analyze whether S10 of merlin is regulating the interaction, a pull-down assay with recombinant merlin fragments and transfected DCAF1 was conducted. Figure 5A shows that a binding site in merlin exists between residues 100 and 314. Mutation of S10 or S518 did not affect the binding affinity of the fragments, showing that these residues are not directly required for binding *in vitro*.

Although S10 is not included in the binding region of DCAF1, co-immunoprecipitation experiments were conducted with full-length proteins to study whether modifications of S10 affect the merlin-DCAF1 association *in vivo*. Merlin S518D associated with DCAF1 stronger than WT did, but interestingly, mutation of S10 significantly decreased the binding of S518D to DCAF1 (Figure 5B). Although S10 is not directly included in the binding region, modifications of this residue can lead to changes, which disrupt the interaction with DCAF1 *in vivo*.

Discussion

The kinase experiments and MS analysis of merlin in this report confirm S10 as a site for Akt-mediated phosphorylation. Within the first 17 amino acids of merlin, several possible phosphorylated residues
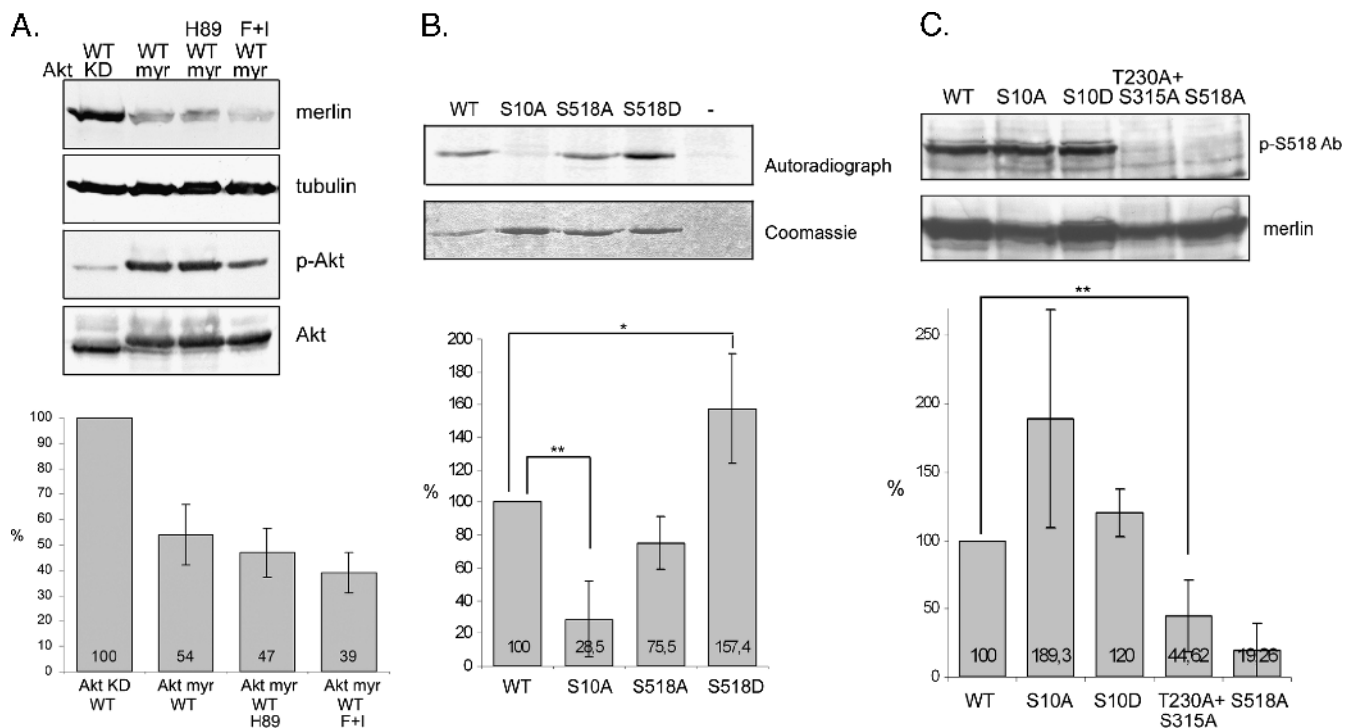
Figure 4. Effect of mutants on merlin phosphorylation. (A) COS-7 cells were cotransfected with merlin WT and Akt KD or Akt myr, and WT + Akt myr–expressing cells were untreated or treated with H89 to inhibit PKA activity or with forskolin and IBMX (F + I) to increase PKA activity. Lysates were detected with merlin A-19 Ab, α-tubulin Ab, phospho-Ser473 Akt Ab (p-Akt), and Akt Ab (upper panels). The merlin amount was quantified, and the level in WT + Akt KD–transfected cells was regarded as 100% (lower chart). Coactivation of Akt and PKA increases merlin degradation. (B) Merlin constructs were expressed in COS-7 cells, immunoprecipitated and phosphorylated *in vitro* using Akt1. The ratio of phospho-signal from autoradiograph normalized to protein amount when WT is 100% is shown in the lower chart. Untransfected cells (−) were used as a negative control. Serine 10 phosphorylation is increased in S518D and decreased in S518A compared with merlin WT. (C) Cell lysates from COS-7 cells transfected with merlin constructs were immunoblotted with merlin phospho-serine 518 antibody (p-S518 Ab) and merlin antibody A-19. The graph illustrates the ratio between merlin S518 phosphorylated over total merlin when WT is regarded as 100%. Serine 518 phosphorylation is significantly decreased in T230A + S315A merlin. **$P < .01$. *$P < .05$.
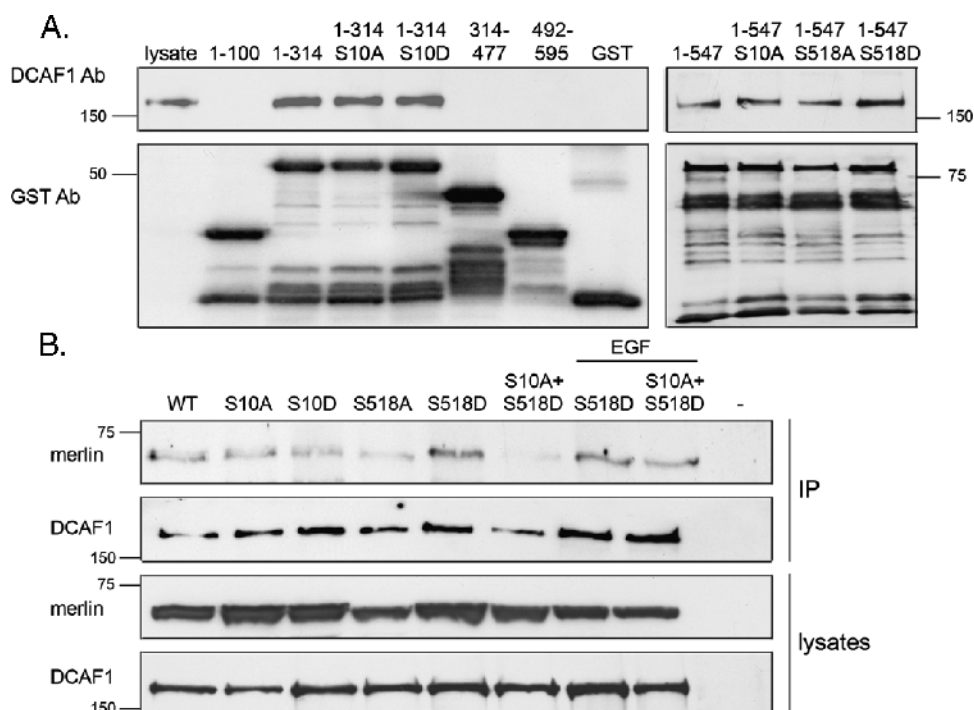
Figure 5. Merlin-DCAF1 interaction *in vitro* and *in vivo*. (A) Glutathione bead–conjugated GST-merlin constructs were incubated with lysates from DCAF1 transfected COS-7 cells, and bound proteins were detected with antibody against DCAF1 (upper panel) and merlin with GST Ab (lower panel). Merlin 1-314 binds DCAF1, whereas 1-100, 314-477, and 492-595 merlin show no binding. Mutation of S10 does not affect the DCAF1 binding affinity of merlin fragments. (B) DCAF1 was immunoprecipitated from merlin and DCAF1-cotransfected COS-7 cell lysates, and merlin was detected with KF10 Ab (upper panel). Equal amounts of proteins were expressed as shown in lysates (lower panels), and untransfected cells (−) were used as control. S518D merlin interacts strongly, whereas S10A + S518D merlin shows reduced binding affinity to DCAF1.

including serine 10 have been predicted based on MS analysis [34], and by using metabolic labeling, we have previously identified S10 as a PKA phosphorylation site [12]. Although S10 serves as a substrate residue for both PKA and Akt, it is not phosphorylated by all AGC kinase family members because S10A mutations do not affect PKC-mediated phosphorylation of merlin. Akt is known to phosphorylate proteins containing the consensus sequence R-X-R-X-X-S/T-F/L, where the arginines at positions −3 and −5 seem to be the most critical [35]. However, S10 is located in a sequence with an arginine at position −2. Also, unconventional Akt phosphorylation sequences have been reported, but they all contain an arginine upstream of the phosphorylated residue [36,37]. The ability of Akt to phosphorylate proteins with arginine in position −2 has not been previously reported, thus merlin represents a novel Akt substrate sequence.

The low levels of merlin in response to coexpression of constitutively active Akt lead us to hypothesize that merlin is degraded in response to Akt phosphorylation, and this was confirmed by mutating S10, which significantly reduced the Akt-induced degradation. We could not detect similar degradation of merlin with the membrane-targeted kinase-dead Akt or in response to EGF treatment as observed when using constitutively active Akt. This suggests that the phosphorylation status of merlin is tightly regulated and that only the active membrane-targeted Akt myr is able to induce the specific and efficient phosphorylation of merlin. Inhibition of the proteasome increased the amount of merlin protein and attenuated Akt-induced degradation, and therefore, we conclude that merlin is degraded in response to S10 phosphorylation through the proteasomal pathway. PKA, which also phosphorylates merlin S10, is not required for Akt-mediated

degradation of merlin, but coactivation of both Akt and PKA has an additive effect on merlin degradation. In accordance, *Nf2* is post-transcriptionally lost in *TEC3KO* mice with increased PKA activity, suggesting that PKA can also regulate the stability of merlin [38].

Akt-mediated phosphorylation of merlin leading to its degradation has previously been described, but the effect was claimed to be mediated through threonine 230 and serine 315 [24]. We could not find an explanation for this discrepancy because all Akt isoforms phosphorylated merlin exclusively on S10; however, it may be explained by different cell lines used and distinct experimental setups. Our results also show that the association of merlin and Akt is direct through at least a strong N-terminal Akt binding site, but phosphorylation of S10 is not required for the merlin-Akt interaction.

To investigate the interplay between the identified functionally important residues in merlin, the phosphorylation of mutated proteins was studied. The assays show that C-terminal S518 phosphorylation of merlin increases N-terminal S10 phosphorylation, suggesting that S518 phosphorylation is the primary event in the functional regulation of merlin. S518 phosphorylation might enhance N-terminal phosphorylation by affecting the intramolecular structure of merlin, as C-terminal phosphorylation is believed to promote a conformational change by disrupting the N- to C-terminal association. However, because S10 is located in the very N-terminal region outside the FERM domain [39,40], it is not determined whether the residue is masked by the C-terminus in the closed conformation. Interestingly, S518 phosphorylation of merlin was significantly decreased in the T230A + S315A construct. Mutation of T230 and S315 has been shown to perturb the intramolecular self-association of merlin [24].
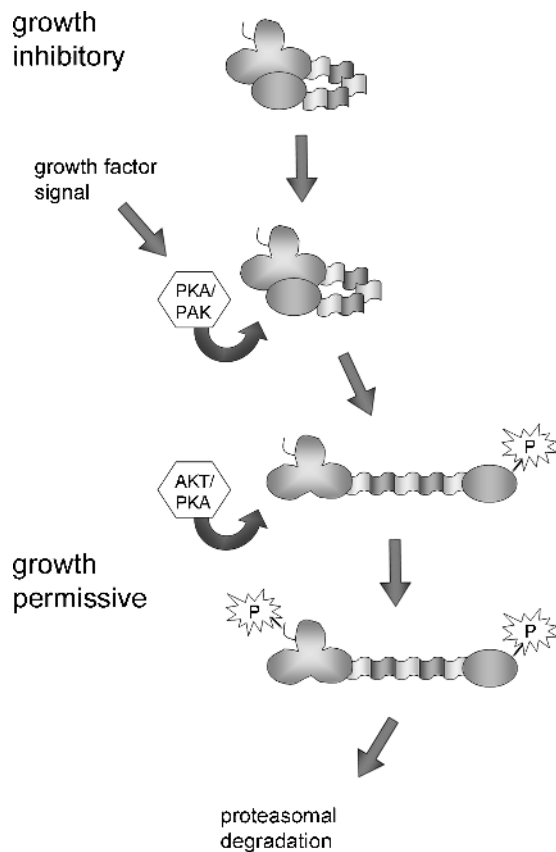
Figure 6. Model of functional inactivation of merlin by two-step phosphorylation. Under growth-inhibitory conditions, unphosphorylated functionally active merlin is in a closed conformation. On growth factor signaling, either PKA or PAK phosphorylates serine 518, leading to a more open conformation. At this conformation, merlin is susceptible to Akt- or PKA-mediated phosphorylation of serine 10, which subsequently triggers degradation and inactivation of merlin through the proteasome pathway.

Thus, disruption of the merlin conformation may affect S518, leading to the decrease in phosphorylation observed. Some of the effects reported for T230 + S315 mutants, such as their impact on apoptosis and cell motility [24,32], might therefore be secondary events resulting from abrogated C-terminal phosphorylation without involving direct Akt-mediated phosphorylation.

Merlin has recently been described to suppress tumorigenesis by translocating to the nucleus to inhibit the E3 ligase CRL4^{DCAF1} [25]. The authors showed that, in the nucleus, merlin functions as a negative regulator of the ligase by inhibiting its ubiquitinating activity. Our data, however, show that modification of S10 affects the merlin-DCAF1 interaction in the soluble fraction of cells, possibly through a conformational transformation of merlin N-terminus, which could target merlin for degradation. This is consistent with the recent data that DCAF1 mediates the degradation of merlin [33]. It remains to be studied whether merlin is a downstream effector of Akt at the membrane but an upstream regulator of DCAF1 in the nucleus.

On the basis of our results and previous studies, we propose a model for a nongenetic mechanism of merlin inactivation (Figure 6). In growth-inhibitory conditions, merlin exists in a closed conformation through N- to C-terminal association, unphosphorylated on serine 518. Growth factor signaling results in phosphorylation of merlin S518 either by PKA or PAK, which renders merlin in an open conformation. This form is subsequently phosphorylated on S10 by either Akt or PKA. Phosphorylation at the N-terminus targets merlin for proteasome-mediated degradation by its DCAF1 interaction or with additional unknown mechanisms. Consequently, merlin's growth-inhibitory function is efficiently inhibited. In accordance with the detected degradation of merlin, coexpression of constitutively active Akt with merlin has been shown to diminish merlin's proapoptotic action [32].

The phosphorylation status of merlin is strictly controlled and compartmentalized because only membrane-targeted constitutively active Akt induces degradation of merlin. The S10-dependent degradation of merlin may occur as a consequence of Akt pathway hyperactivation, a common feature in malignant neoplasias. Although difficult to unequivocally confirm, we postulate that temporal transient phosphorylation of S10 regulates the cytoskeletal functions of merlin [12], whereas constitutive phosphorylation in malignant cells leads to merlin degradation. Further studied are needed to determine whether Akt-mediated S10 phosphorylation plays a role in the normal functional regulation of merlin or whether it is just a consequence of Akt overactivation in neoplasia.

Multiple tumor types harbor mutations in components of the PI3K/Akt pathway leading to increased Akt signaling [13], and mutations and loss of merlin expression have been reported in several tumor types in addition to those associated with NF2 [41,42]. For example, in malignant gliomas, merlin expression is reduced [43], and the PI3K signaling pathway is activated [44]. Recently, a compound targeting the Akt pathway was investigated as a chemotherapeutic in preclinical studies for vestibular schwannomas, tumors associated with NF2 [45]. It remains to be seen whether inactivation of this pathway will reduce tumor cell growth and have therapeutic potential for patients with NF2.

In conclusion, our results suggest that degradation of the tumor suppressor merlin is enhanced as a consequence of overactivation of the Akt pathway and hence merlin phosphorylation. Activation of the PI3K/Akt pathway could therefore represent a novel way to inactivate merlin in tumors that lack *NF2* mutations.

Acknowledgments

References

[1] McClatchey AI and Giovannini M (2005). Membrane organization and tumorigenesis—the NF2 tumor suppressor, merlin. *Genes Dev* **19**, 2265–2277.

[2] McClatchey AI and Fehon RG (2009). Merlin and the ERM proteins—regulators of receptor distribution and signaling at the cell cortex. *Trends Cell Biol* **19**, 198–206.

[3] Sherman L, Xu HM, Geist RT, Saporito-Irwin S, Howells N, Ponta H, Herrlich P, and Gutmann DH (1997). Interdomain binding mediates tumor growth suppression by the *NF2* gene product. *Oncogene* **15**, 2505–2509.

[4] Gutmann DH, Haipek CA, and Hoang Lu K (1999). Neurofibromatosis 2 tumor suppressor protein, merlin, forms two functionally important intramolecular associations. *J Neurosci Res* **58**, 706–716.

[5] Grönholm M, Sainio M, Zhao F, Heiska L, Vaheri A, and Carpén O (1999). Homotypic and heterotypic interaction of the neurofibromatosis 2 tumor suppressor protein merlin and the ERM protein ezrin. *J Cell Sci* **112**, 895–904.

[6] Shaw RJ, Paez JG, Curto M, Yaktine A, Pruitt WM, Saotome I, O'Bryan JP, Gupta V, Ratner N, Der CJ, et al. (2001). The Nf2 tumor suppressor, merlin, functions in *rac*-dependent signaling. *Dev Cell* **1**, 63–72.

[7] Kissil JL, Johnson KC, Eckman MS, and Jacks T (2002). Merlin phosphorylation by p21-activated kinase 2 and effects of phosphorylation on merlin localization. *J Biol Chem* **277**, 10394–10399.

[8] Xiao GH, Beeser A, Chernoff J, and Testa JR (2002). p21-activated kinase links Rac/Cdc42 signaling to merlin. *J Biol Chem* **277**, 883–886.

[9] Alfthan K, Heiska L, Grönholm M, Renkema GH, and Carpén O (2004). Cyclic AMP-dependent protein kinase phosphorylates merlin at serine 518 independently of p21-activated kinase and promotes merlin-ezrin heterodimerization. *J Biol Chem* **279**, 18559–18566.

[10] Morrison H, Sherman LS, Legg J, Banine F, Isacke C, Haipek CA, Gutmann DH, Ponta H, and Herrlich P (2001). The NF2 tumor suppressor gene product, *merlin*, mediates contact inhibition of growth through interactions with CD44. *Genes Dev* **15**, 968–980.

[11] Jin H, Sperka T, Herrlich P, and Morrison H (2006). Tumorigenic transformation by CPI-17 through inhibition of a merlin phosphatase. *Nature* **442**, 576–579.

[12] Laulajainen M, Muranen T, Carpén O, and Grönholm M (2008). Protein kinase A–mediated phosphorylation of the NF2 tumor suppressor protein merlin at serine 10 affects the actin cytoskeleton. *Oncogene* **27**, 3233–3243.

[13] Vivanco I and Sawyers CL (2002). The phosphatidylinositol 3-kinase AKT pathway in human cancer. *Nat Rev Cancer* **2**, 489–501.

[14] Franke TF (2008). PI3K/Akt: getting it right matters. *Oncogene* **27**, 6473–6488.

[15] Alessi DR, James SR, Downes CP, Holmes AB, Gaffney PR, Reese CB, and Cohen P (1997). Characterization of a 3-phosphoinositide–dependent protein kinase which phosphorylates and activates protein kinase Bα. *Curr Biol* **7**, 261–269.

[16] Alessi DR, Andjelkovic M, Caudwell B, Cron P, Morrice N, Cohen P, and Hemmings BA (1996). Mechanism of activation of protein kinase B by insulin and IGF-1. *EMBO J* **15**, 6541–6551.

[17] Li Y, Tennekoon GI, Birnbaum M, Marchionni MA, and Rutkowski JL (2001). Neuregulin signaling through a PI3K/Akt/Bad pathway in Schwann cell survival. *Mol Cell Neurosci* **17**, 761–767.

[18] Fraenzer JT, Pan H, Minimo L Jr, Smith GM, Knauer D, and Hung G (2003). Overexpression of the *NF2* gene inhibits schwannoma cell proliferation through promoting PDGFR degradation. *Int J Oncol* **23**, 1493–1500.

[19] Rong R, Tang X, Gutmann DH, and Ye K (2004). Neurofibromatosis 2 (NF2) tumor suppressor merlin inhibits phosphatidylinositol 3-kinase through binding to PIKE-L. *Proc Natl Acad Sci USA* **101**, 18200–18205.

[20] Jacob A, Lee TX, Neff BA, Miller S, Welling B, and Chang LS (2008). Phosphatidylinositol 3-kinase/AKT pathway activation in human vestibular schwannoma. *Otol Neurotol* **29**, 58–68.

[21] Ammoun S, Flaiz C, Ristic N, Schuldt J, and Hanemann CO (2008). Dissecting and targeting the growth factor–dependent and growth factor–independent extracellular signal–regulated kinase pathway in human schwannoma. *Cancer Res* **68**, 5236–5245.

[22] Hilton DA, Ristic N, and Hanemann CO (2009). Activation of ERK, AKT and JNK signalling pathways in human schwannomas *in situ*. *Histopathology* **55**, 744–749.

[23] Altomare DA, Vaslet CA, Skele KL, De Rienzo A, Devarajan K, Jhanwar SC, McClatchey AI, Kane AB, and Testa JR (2005). A mouse model recapitulating molecular features of human mesothelioma. *Cancer Res* **65**, 8090–8095.

[24] Tang X, Jang SW, Wang X, Liu Z, Bahr SM, Sun SY, Brat D, Gutmann DH, and Ye K (2007). Akt phosphorylation regulates the tumour-suppressor merlin through ubiquitination and degradation. *Nat Cell Biol* **9**, 1199–1207.

[25] Li W, You L, Cooper J, Schiavon G, Pepe-Caprio A, Zhou L, Ishii R, Giovannini M, Hanemann CO, Long SB, et al. (2010). Merlin/NF2 suppresses tumorigenesis by inhibiting the E3 ubiquitin ligase CRL4(DCAF1) in the nucleus. *Cell* **140**, 477–490.

[26] den Bakker MA, Tascilar M, Riegman PH, Hekman AC, Boersma W, Janssen PJ, de Jong TA, Hendriks W, van der Kwast TH, and Zwarthoff EC (1995). Neurofibromatosis type 2 protein co-localizes with elements of the cytoskeleton. *Am J Pathol* **147**, 1339–1349.

[27] O'Connell KL and Stults JT (1997). Identification of mouse liver proteins on two-dimensional electrophoresis gels by matrix-assisted laser desorption/ionization mass spectrometry of *in situ* enzymatic digests. *Electrophoresis* **18**, 349–359.

[28] Shevchenko A, Wilm M, Vorm O, and Mann M (1996). Mass spectrometric sequencing of proteins silver-stained polyacrylamide gels. *Anal Chem* **68**, 850–858.

[29] Nyman TA, Rosengren A, Syyrakki S, Pellinen TP, Rautajoki K, and Lahesmaa R (2001). A proteome database of human primary T helper cells. *Electrophoresis* **22**, 4375–4382.

[30] Ohman T, Lietzen N, Valimaki E, Melchjorsen J, Matikainen S, and Nyman TA (2010). Cytosolic RNA recognition pathway activates 14-3-3 protein mediated signaling and caspase-dependent disruption of cytokeratin network in human keratinocytes. *J Proteome Res* **9**, 1549–1564.

[31] Brazil DP, Park J, and Hemmings BA (2002). PKB binding proteins. Getting in on the akt. *Cell* **111**, 293–303.

[32] Okada M, Wang Y, Jang SW, Tang X, Neri LM, and Ye K (2009). Akt phosphorylation of merlin enhances its binding to phosphatidylinositols and inhibits the tumor-suppressive activities of merlin. *Cancer Res* **69**, 4043–4051.

[33] Huang J and Chen J (2008). VprBP targets merlin to the Roc1-Cul4A-DDB1 E3 ligase complex for degradation. *Oncogene* **27**, 4056–4064.

[34] Cole BK, Curto M, Chan AW, and McClatchey AI (2008). Localization to the cortical cytoskeleton is necessary for Nf2/merlin–dependent epidermal growth factor receptor silencing. *Mol Cell Biol* **28**, 1274–1284.

[35] Alessi DR, Caudwell FB, Andjelkovic M, Hemmings BA, and Cohen P (1996). Molecular basis for the substrate specificity of protein kinase B; comparison with MAPKAP kinase-1 and p70 S6 kinase. *FEBS Lett* **399**, 333–338.

[36] Basu S, Totty NF, Irwin MS, Sudol M, and Downward J (2003). Akt phosphorylates the yes-associated protein, YAP, to induce interaction with 14-3-3 and attenuation of p73-mediated apoptosis. *Mol Cell* **11**, 11–23.

[37] Chen Q, Powell DW, Rane MJ, Singh S, Butt W, Klein JB, and McLeish KR (2003). Akt phosphorylates p47[phox] and mediates respiratory burst activity in human neutrophils. *J Immunol* **170**, 5302–5308.

[38] Jones GN, Tep C, Towns WH II, Mihai G, Tonks ID, Kay GF, Schmalbrock PM, Stemmer-Rachamimov AO, Yoon SO, and Kirschner LS (2008). Tissue-specific ablation of Prkar1a causes schwannomas by suppressing neurofibromatosis protein production. *Neoplasia* **10**, 1213–1221.

[39] Brault E, Gautreau A, Lamarine M, Callebaut I, Thomas G, and Goutebroze L (2001). Normal membrane localization and actin association of the NF2 tumor suppressor protein are dependent on folding of its N-terminal domain. *J Cell Sci* **114**, 1901–1912.

[40] Shimizu T, Seto A, Maita N, Hamada K, Tsukita S, Tsukita S, and Hakoshima T (2002). Structural basis for neurofibromatosis type 2. Crystal structure of the merlin FERM domain. *J Biol Chem* **277**, 10332–10336.

[41] Bianchi AB, Hara T, Ramesh V, Gao J, Klein-Szanto AJ, Morin F, Menon AG, Trofatter JA, Gusella JF, and Seizinger BR (1994). Mutations in transcript isoforms of the *neurofibromatosis 2* gene in multiple human tumour types. *Nat Genet* **6**, 185–192.

[42] Sekido Y, Pass HI, Bader S, Mew DJ, Christman MF, Gazdar AF, and Minna JD (1995). *Neurofibromatosis type 2* (*NF2*) gene is somatically mutated in mesothelioma but not in lung cancer. *Cancer Res* **55**, 1227–1231.

[43] Lau YK, Murray LB, Houshmandi SS, Xu Y, Gutmann DH, and Yu Q (2008). Merlin is a potent inhibitor of glioma growth. *Cancer Res* **68**, 5733–5742.

[44] Lassman AB (2004). Molecular biology of gliomas. *Curr Neurol Neurosci Rep* **4**, 228–233.

[45] Lee TX, Packer MD, Huang J, Akhmametyeva EM, Kulp SK, Chen CS, Giovannini M, Jacob A, Welling DB, and Chang LS (2009). Growth inhibitory and anti-tumour activities of OSU-03012, a novel PDK-1 inhibitor, on vestibular schwannoma and malignant schwannoma cells. *Eur J Cancer* **45**, 1709–1720.